Received September 1, 2020, accepted September 20, 2020, date of publication September 23, 2020,
date of current version October 6, 2020.

Digital Object Identifier 10.1109/ACCESS.2020.3026136

Risk Assessment of Polluted Glass Insulator Using Leakage Current Index Under Different Operating Conditions

ALI AHMED SALEM[1], (Member, IEEE), RAHISHAM ABD-RAHMAN[1], (Member, IEEE), SAMIR AHMED AL-GAILANI[2], (Member, IEEE), ZAINAL SALAM[3], MUHAMMAD SAUFI KAMARUDIN[1], (Member, IEEE), HIDAYAT ZAINUDDIN[4], (Member, IEEE), AND MOHD FAIROUZ MOHD YOUSOF[1], (Member, IEEE)

[1]Faculty of Electrical and Electronic Engineering, Universiti Tun Hussein Onn Malaysia, Batu Pahat 86400, Malaysia
[2]School of Electrical and Electronic Engineering, Universiti Sains Malaysia, Penang 14300, Malaysia
[3]Faculty of Engineering, School of Electrical Engineering, Universiti Teknologi Malaysia, Johor Bahru 81310, Malaysia
[4]Faculty of Electrical Engineering, Universiti Teknikal Malaysia Melaka (UTeM), Durian Tunggal 76100, Malaysia

Corresponding authors: Samir Ahmed Al-Gailani (samer.algailani@usm.my) and Ali Ahmed Salem (en.alisalem@gmail.com)

This work was supported in part by the Universiti Tun Hussein Onn Malaysia and the Ministry of Higher Education, Malaysia, under Grant U117, and in part by the University of Science, Malaysia, under Grant 304/PELECT/6315344.

ABSTRACT In this article, an innovative approach to assess the risk of uniform/non-uniform pollution and wet high voltage glass insulator is proposed. The assessment is based on a new index, named as R_{hi}, which is derived from the 3rd, 5th and 7th harmonics of the leakage current. Two 33 kV strings of cap and pin glass insulators having three units with different profiles are employed to evaluate the risk level, based on measured critical voltage gradient (Ec). Critical voltage stress tests are executed on the contaminated insulators under different ratios of lower to upper surface (J) and wetting rates. Furthermore, the effects of ratio of soluble deposit density ($ESDD$) to non-soluble deposit density ($NSDD$) on the flashover occurrence are analyzed. It was found that the insulator profile has significant influences on the likelihood of flashover which is estimated as 38% and 24% for type A and B insulators, respectively. From the results, it can be concluded that the proposed R_{hi} index is able to predict the risk level of the insulator and the probability of flashover occurrence more accurately than the 5th/3rd index, which is widely published in literature.

INDEX TERMS Polluted insulators, risk assessment, leakage current harmonics, fast Fourier transform, glass insulator.

I. INTRODUCTION

Outdoor insulator is one of the critical equipment's of power system transmission and distribution. It is used to insulate the conductor from the grounded tower and to assist the power lines with mechanical support. The performances of outdoor insulator are significantly affected by different mechanical and environmental factors like the type of material, installation arrangement, and degree of contamination on its surface [1]–[5]. The contaminated environment causes the insulators to be susceptible to high magnitude of leakage current and increases the arc activities over its surface. These conditions may result in the undesirable flashover phenomenon, which in turn, triggers an interruption in the power transmission [6]–[10]. Therefore, to overcome this fact, monitoring the leakage currents becomes an important preventive aspect to ensure the overall health of the insulator. The deposited surface pollutant such as dust and chemical emission is one of the biggest threats faced by outdoor insulators. Arcing and corona activities change the insulator surface characteristics, which can lead to premature ageing of insulators [11]–[14]. In addition, the surface tracking and erosion leads to material degradation. All these phenomena increase the magnitude of leakage current (LC) flow over the insulator surface. Thus, the assessment of outdoor insulator properties and its long-term performance is a hot topic for investigation by many researcher [15]–[21]. One particularly issue of interest is that to establish an accurate relationship between the LC and pollution severity while the insulator is in service. Authors in [22]–[24] have predicted the pollution

The associate editor coordinating the review of this manuscript and approving it for publication was Byung-Gyu Kim.

severity by analysing the statistical values of the LC such as the mean, maximum and the standard deviation (STD). Using these parameters, the dimensions and severity of the pollution layer is estimated. In another approach [25], the phase shift angle between the Leakage currents and voltage signal is investigated to predict the contamination severity. The result indicates that the variations in the cosine of the phase angle (displacement factor) is a good indicator to determine the pollution on insulator surface [25]. Independent findings produced by several authors in [26] have shown that the flashover measurement approach can be used to access the contamination severity on insulator. However, certain prior knowledge on the parameters such as the dry bands are needed. Another interesting approach to predict the pollution severity is by using a technique known as the LC extraction. This concept was utilized and suggested by several researchers [27], [28].

The LC of insulators are analyzed in the frequency domains using Fast Fourier Transform (FFT); from the frequency content, it was concluded that the presence of LC can be quantified by measuring its odd harmonic components. For the 50 Hz system, the harmonics of concern are third (150 Hz) and fifth (250 Hz) [28]. This intensification of these harmonics increases the total harmonic distortion (THD) that varies depending on pollution level [29]. Based on this observation, an index that reflects the health condition of the insulators was suggested by [30]–[32]. Further, authors in [32] used the frequency components decomposition concept to propose the fifth to third harmonics ratio (which will be subsequently the 5th/3rd index) of LC to predict flashovers occurrences. The reported results on silicon rubber and porcelain insulators indicated that the pollution severity is closely related to the value of this ratio. Similarly, authors in [31], confirmed that the 5th/3rd index is capable of assessing the flashover occurrence probability.

Despite the promising results using the 5th/3rd index, a question can be raised whether the inclusion of higher order harmonics in the index improves the prediction accuracy. This is a legitimate proposal because not much additional effort is required to obtain the seventh harmonic using the existing LC monitoring system. It would be interesting to know if a new formulation of the harmonics ratio can produce a better result than the 5th/3rd index. Based on this hypothesis, an alternative index is proposed to assess the risk status of strings glass insulators. The new indicator, named as R_{hi} is formulated from 3rd, 5th and 7th harmonic components of the LC. To verify the effectiveness of this new index, a 33 kV Insulator string has been tested experimentally under different contamination conditions. These include the wetting condition and soluble deposit density to non-soluble deposit density ratio. Both of the normal and probability distribution functions (PFD) were used to calculate the insulator strings risk. The impacts of profile on the flashover voltage gradient *Ec* and degree of flashover occurrence probability are also analyzed. This study can be effectively used to monitor and diagnose the risk level of in-situ string insulators without performing pollution measurement over the insulator surface directly.

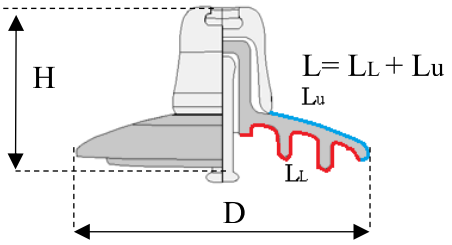

FIGURE 1. Schematic of the insulator.

TABLE 1. Tested insulators parameters.

Insulator Type	A	B
Insulator height H (cm)	14.6	14.6
Diameter D (cm)	25.5	28
Leakage distance L (cm)	32	34
Length of lower side L_L (cm)	20.5	21.5
Length of upper side L_u (cm)	11.5	12.5

II. METHOD AND MATERIALS

A. EXPERIMENT SETUP AND TEST SPECIMENS

Two insulator strings with different geometric structures were selected in this test. They are denoted by Type A and B, respectively. Their specifications are listed and tabulated in Figure 1and Table 1. Figure 2(a) illustrates the experimental high voltage setup layout diagram for the insulators under test. A pictorial view of the setup and the equipment are shown in Figure 2(b). It comprises of a HV transformer to energize the insulators (220 kV, 5 kVA, and 50 Hz f), a protective resistance (2400 ohm), a capacitor divider (100, 25.000 pf) and a leakage current and flashover voltage gradient measuring unit. The experiment is set to comply with the IEC 60507 standard. A steam generator device and the wetting rate controller were used to simulate the wetting process of the specimens.

B. ARTIFICIAL POLLUTION AND WETTING

First, the specimens (i.e. the insulators under test) were thoroughly cleaned using alcohol and tap water to ensure that they were completely free of dirt and traces of grease. Then the insulators were left to dry up naturally.

Contamination layer was formed uniformly as well as non-uniformly on the surface of the insulators under test using the solid layer approach. In this method, three pollution slurry was prepared with different non-soluble deposit density (*NSDD*). The former used Kaolin at 10, 40 and 120 g, mixed with one liter of distilled water and an appropriate amount of NaCl (common salt), according to the *ESDD* (mg/cm^2) severity required. The contamination severity is categorized into four levels of pollution based on *ESDD* value as: low (0.03 mg/cm^2), moderate (0.09 mg/cm^2), high (0.15 mg/cm^2) and severe (0.24 mg/cm^2). This categorization

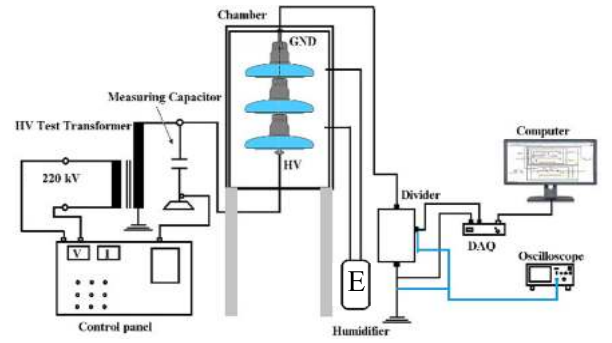

(a)

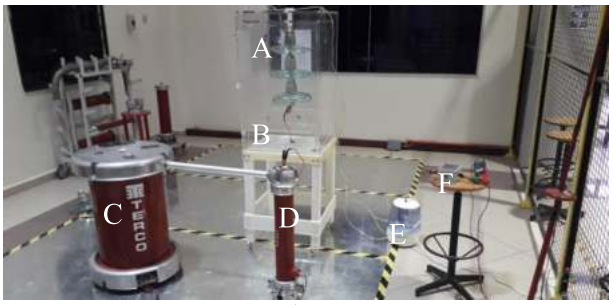

(b)

FIGURE 2. (a) Schematic diagram of the experiment setup (b) The pictorial view of the setup. Component labels: A: the tested samples, B: chamber, C: transformer, D: capacitor, E: fog generator and F: potential divider.

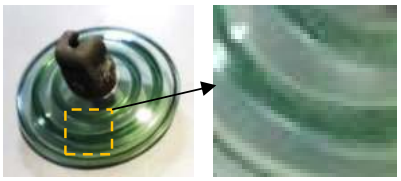

Clean insulator

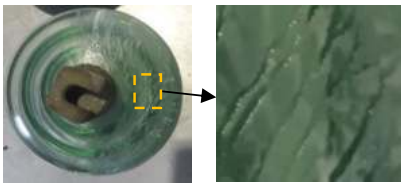

Polluted insulator

FIGURE 3. Clean and polluted glass insulator.

is in compliance with IEC 60507. Figure 3 shows the insulator sample under contaminated and clean conditions.

Next, the completely dried insulator was suspended in an artificial test chamber, whose walls are made up of polycarbonate material. The dimensions of its walls are 50 x 50 x 75 cm. The insulator under test was sprayed simultaneously with high pressure water and fog using an air-water compressor and fog generator. To produce wetting, eight nozzles were mounted all along the chamber's inner walls. The nozzles were fed from an air-water compressor using high pressure pipelines. The insulator under test was wetted with three levels of clean fog namely; mild, medium and high. The approximate wetting rate of 2.5 ± 0.1 l/ h, 5 ± 0.2 l / h and 7.5 ± 0.3 l / h, respectively was achieved. The temperature of a chamber was adjusted between 27 and 30°C. The relative humidity of the fog generator varied between 81% and 85%. The atmospheric pressure is kept to approximately 101 kPa.

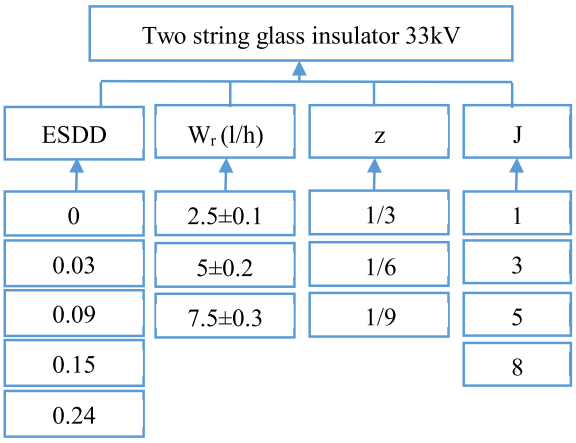

FIGURE 4. Operating conditions for tested string insulators.

C. FLASHOVER STRESS MEASUREMENT

The flashover voltage stress test was conducted under variation operating conditions as detailed in Figure 4. The energized voltage was increased at a rate of 3 kV/s. The flashover tests in each wetting rate and contamination level were performed at least 4 times, with 3 min intervals. The average flashover voltage stress (E_c) and for four tests can be evaluated as,

$$E_c = \frac{1}{4}\sum_{i=1}^{4} E_i \tag{1}$$

$$E_c = U_c/L \tag{2}$$

while the standard deviation ($\sigma\%$) of flashover voltage stress is computed as

$$\sigma\% = 1/E_c\sqrt{\sum_{i=1}^{4}(E_i - E_c)^2/3} \times 100 \tag{3}$$

which Ei is i^{th} flashover voltage stress and L is creepage distance.

D. POLLUTION SEVERITY (ESDD) CALCULATION

To measure the equivalent salt deposit density (*ESDD*) of the contamination layer on the under-test insulator surface, the pollution was carefully extracted from the surface of the insulator (except for metal parts). The extracted pollution was then dissolved in 0.5-litre deionized water. Next, using a conductivity meter HI8733, the conductivity of the solution was measured at room temperature with correction factor ($b = 0.0228$). In this case, the salinity (Sa) of the solution was expressed according to IEC 60507 standard by (6). Based on the measured conductivity at the room temperature, the conductivity at 20°C have been given as in (5) and *ESDD* in (mg/cm^2) can be calculated as in (7),

$$b = 0.9 \times 10^{-5}\theta^2 - 0.8 \times 10^{-3}\theta + 0.0353 \tag{4}$$

$$\sigma_{20} = \sigma_\theta \times [1 - b(\theta - 20)] \quad (5)$$

$$S_a = 5.7 \times (\sigma_{20})^{1.03} \quad (6)$$

$$ESDD = (S_a \times V)/A \quad (7)$$

where $\sigma_{20}, \sigma_\theta, \theta, A$ postulate the conductivity of the pollution layer (S/m)at 20°C, the volume conductivity at θ, the solution temperature (°C), and the insulator surface area (cm^2). As can be observed, Sa represents the salinity of the solution (kg/m^3), V is the volume of the solution (cm^3), and b is the factor depending on temperature θ.

In case non-uniform pollution distribution,the average of ESDD of top and bottom of insulator surface can be satisfied as,

$$ESDD_{av} = (ESDD_U \cdot S_U + ESDD_L \cdot S_L)/(S_U + S_L) \quad (8)$$

$$J = ESDD_L/ESDD_U \quad (9)$$

where $ESDD_U$ and $ESDD_L$ are the salt deposit density of the upper and lower surfaces of the insulators, respectively. In addition, S_U and S_L are the upper and lower surface areas of the insulators, respectively. The *NSDD* was determined based on the following formula [33]:

$$NSDD = [(w_f - w_i) \times 10^3]/A(\mathrm{mg/cm^2}) \quad (10)$$

wf, wi, and *A* are the weight of the filter paper containing pollutants in g, the initial weight of the filter paper under dry conditions in g, and the insulator surface area. The ratio of non-soluble deposit density (*NSDD*) to soluble deposit deposit (*ESDD*) has been expressed in (11) as,

$$z = ESDD/NSDD \quad (11)$$

E. LEAKAGE CURRENT MEASUREMENT

As it can be seen in the experiment setup layout given in (Figure 2) above, the voltage divider (104:1) between the upper insulator cap and the ground electrode was used to measure the LC of the contaminated string insulators. This voltage divider was connected into the circuit to produce low voltage for the monitoring and measuring equipment safety which can lower the measured data values using the DAQ card NI6024E within permissible input voltage range of ±10 V. In this respect, it should be observed that the monitoring system consists other unit addition to measurement hardware unit, namely software unit. This unit is used to transfer data from the DAQ NI6024E, save, and then display it on a LabVIEW graphical interface. In the present work, LabVIEW software was used for the implementation of the supervisory system software interface. The current session GUI displays the time of LC evolution, the voltage applied and the spectrum analysis is shown in Figure 5.

III. RESULT AND DISCUSSION

A. LEAKAGE CURRENT CHARACTERISTICS UNDER OPERATING CONDITION

The further analysis of the leakage current was experimentally measured. The characteristics of LC such as peak value, harmonic components, harmonics index of the LC signal for the insulators were evaluated reliably to identify the

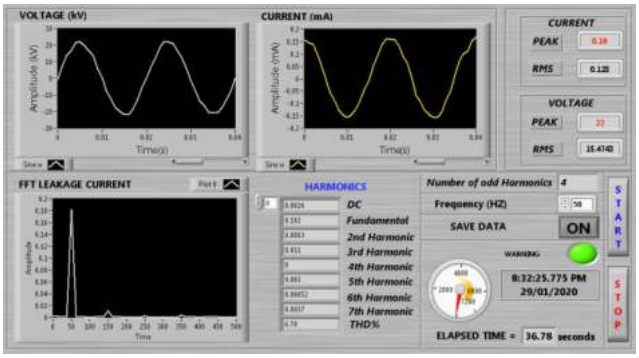

FIGURE 5. The LabVIEW GUI for the experimental set-up.

situation of the insulator and to predict the occurrence of flashover or risk usage according to the conduction of the leakage current. Figure 6 elucidates leakage current characteristics for the insulator A (as a sample insulator) at various contamination levels in wetting rates of 2.5 ± 0.1 l/h, z equal to 1/3 and J equal to 1:1 under 33 kV. From Figure 6, it can be noted that the value of the fundamental harmonic component of the LC increases considerably with the increase in the contamination level. Meanwhile, the third harmonic of the LC of tested insulators appears to be lower than the fifth component in the clean condition and the lower pollution degree and low wetting rate as well. On the other hand, a huge change in the components (3^{rd}, 5^{th}, and 7^{th}) can be noticed when fog is applied and increase the wetting rate on the polluted insulators surfaces. The third harmonic will escalate until it exceeds the fifth harmonic with increasing pollution and wetness, while the seventh harmonic value will increase and become approximately equal to the amount of third harmonic as shown in Figure 7. The 3^{rd} harmonic has significant increase in partial arc cases compared to 5^{th} and 7^{th} components, it reached close to 40% of the fundamental component according to [34].

B. LEAKAGE CURRENT INDEX, R_{HI}

Insulators monitoring based on leakage current depends mainly on the shape of the leakage current waveform. There is a nonlinear impedance of the pollution layer on the insulator surface.

Pollution of the surface and moistening boosts the conductivity of the pollution layer and thus the leakage current will be increased. Because of this nonlinear impedance, the sinusoidal wave of current is distorted. Otherwise, the rise in value of LC creates dry bands and results in small discharges which distorts the current waveform. The leakage current of the non-sinusoidal wave reflects the presence of the 3^{rd} harmonic content, the 3^{rd} component increases with increasing the contamination to exceed the 5^{th} and 7^{th} components. This phenomenon has also been observed in laboratory experiments. Accordingly, variations of odd harmonics of leakage current (3^{rd}, 5^{th}, and 7^{th}) are a criterion for assessing the service condition of the tested insulators So, to propose criterion for monitoring insulator status, will be considered the odd harmonics components up to 7^{th} component

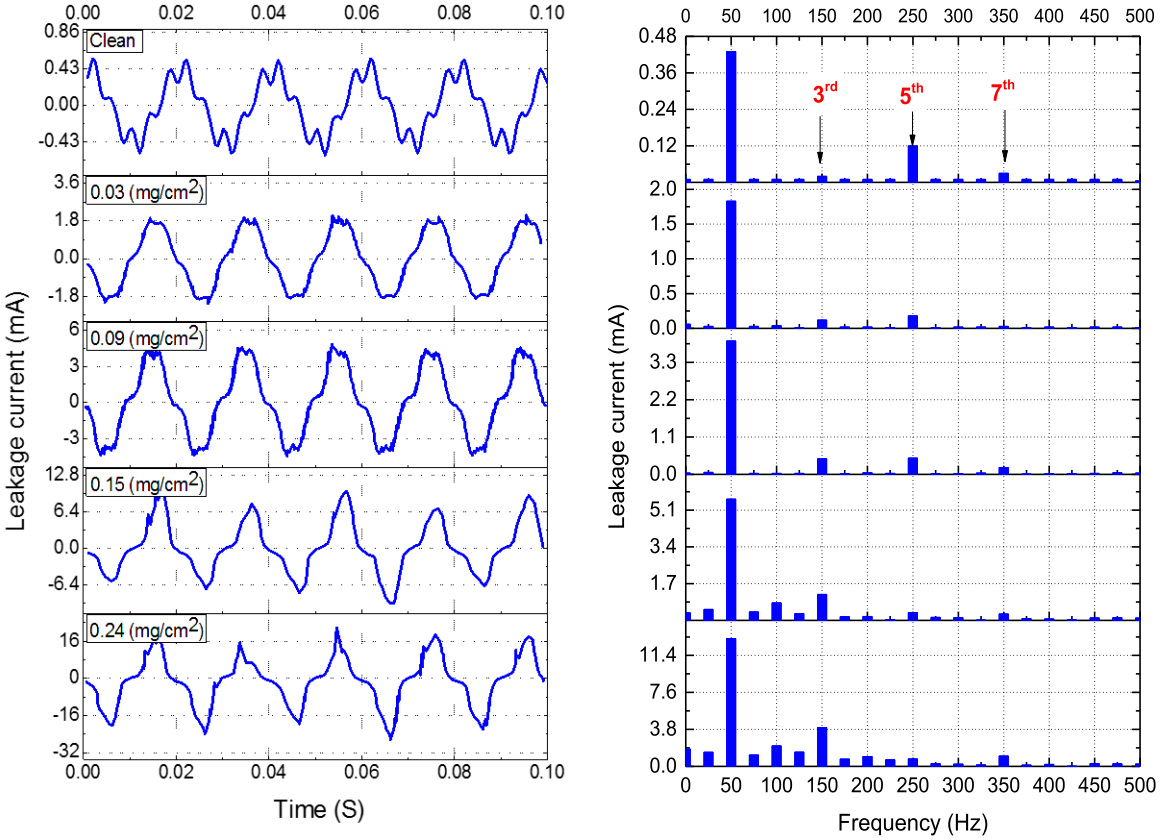

FIGURE 6. Leakage current time and frequency characteristics for the insulator A at various contamination in z = 1/3 and J = 1:1 under wetting rate of 2.5 ± 0.2 l/h and applied voltage of 33 kV.

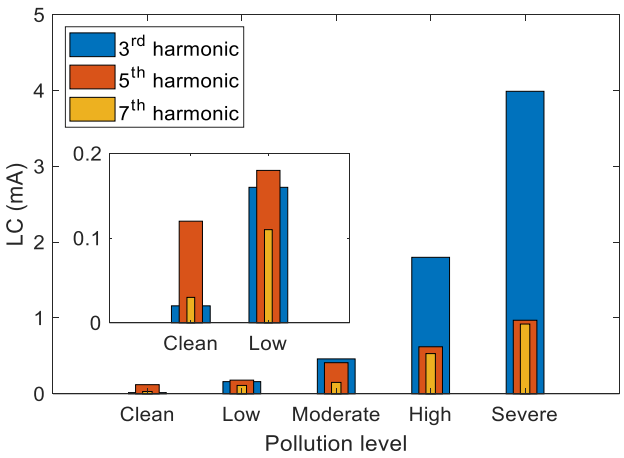

FIGURE 7. Leakage current odd harmonics under different contamination levels.

of leakage current measured from the tested insulators to formulate the index as:

$$R_{hi} = I_3/(I_5 + I_7) \tag{12}$$

I_3, I_5 and I_7 represent the amplitude of 3rd, 5th and 7th harmonics components of leakage current the general description of signal of the leakage current harmonics component is formulated as:

$$I_h = I_{mh} \sin(2\pi(h \times f_F)t + \phi_h) \quad h = 3, 5, 7 \tag{13}$$

I_h is current of h^{th} harmonic, I_{mh} is harmonic component amplitude, Φ_h is phase angle between fundamental and harmonic component, f_F is frequency system which equal to 50 Hz and h is harmonic number, respectively. As a result of the above fact, the new indicator is suitable for use as the criterion for assessing the risk state of insulators in-service conditions. In this work, the proposed index as well as third to fifth ratio index have been calculated, to enable us to compare between the two indices. Table 2 and Figure 8 show the comparison of third to fifth ratio and the proposed index (R_{hi}) values using obtained experiment data insulator type A as sample under variation of *ESDD* and wetting rate of 2.5+0.1 l/h. According to the results produced which are demonstrated in Table 2 and Figure 8, it can be concluded that the 3rd/5th index does not tend steadily and becomes less accurate as a monitoring indicator. Whereas, the proposed LC index remains fairly stable under constant *ESDD*, an increase in the *ESDD* is accompanied by an increase in R_{hi}, making it a more reliable index for insulator monitoring.

C. CORRELATION BETWEEN ESDD AND LC INDEX

Table 3 shows the results of the new indicator extracted from the leakage current odd harmonics components of the tested insulator strings under various pollution levels uniformly and non-uniformly (1:5 as example). These components are used as a tool in the estimation of the contamination

TABLE 2. $3^{rd}/5^{th}$ ratios and R_{hi} comparison for insulator type A.

ESDD (mg/cm^2)	Harmonics components			3rd/5th	Rhi
	3rd	5th	7th		
0.03	0.01	0.12	0.03	0.61	0.55
0.06	0.16	0.18	0.11	0.24	0.90
0.15	0.46	0.41	0.15	0.85	1.57
0.24	1.8	0.62	0.53	0.54	2.68

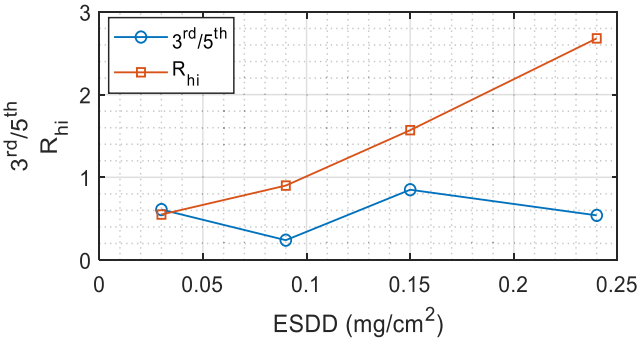

FIGURE 8. Comparison of $3^{rd}/5^{th}$ ratios and R_{hi} for insulator type A under different ESDD and 2.5 ± 0.1 l/h.

level and predict the phases under risk for polluted insulator strings.

Figure 10 illustrates the R_{hi}- ESDD curve obtained for each of the insulator strings under operating condition which is used to investigate the correlation between contamination severity and LC index (R_{hi}). It can be observed from Table 3 and Table 4 that, as the ESDD raises, the R_{hi} increases linearly. Referring to Table 3, Table 4 and Figure 9, it can be clearly seen that any change in contamination severity has considerable impact on the LC index value. Under certain J and W_r values, the R_{hi} value has increased with an increment of ESDD in all cases. For instance, when $J = 5$ and $W_r = 2.5 \pm 0.1$ l/h, by increasing the *ESDD* from 0.03 to 0.09 and 0.24 mg/cm^2 for the insulator string type A under uniform pollution, the R_{hi} has increased by 92.1% and 428.9%, respectively. Accordingly, by increasing the *ESDD* level, the LC index is raised which indicates to increase the possibility of occurrence of the flashover on contaminated insulators.

Figure 9 (a) represents the experimental data of R_{hi}-*ESDD* with variation on wetting rate. To establish the correlation between the proposed index and pollution severity, the linear least squares algorithm has been used to fit the data extracted from the experiment. As shown in Figure 9(a), the wetting rate has a mid-effect on the LC index of insulator string type A. Thus, with different fog input rate under pollution conditions results in different wetting effects on the insulator The LC index rises with the increase in W_r. for example, under different values of W_r, when $J = 5$, $ESDD = 0.24$ mg/cm^2 and if wetting rate is increased from $W_r = 2.5 \pm 0.1$ l/h to 5 ± 0.2 l/h and 7.5 ± 0.3 l/h, the R_{hi} raises by 4.9% and 10.5%, respectively. The relation between LC index R_{hi} and contamination severity under uneven pollution degree J is presented in Figure 9 (b). It is clear that the

TABLE 3. LC index result under different uniform pollution, z and W_r.

			ESDD (mg/cm^2)				
Ins	z	W_r (l/h)	0	0.03	0.09	0.15	0.24
A		2.5±0.1	0.033	0.55	0.84	1.57	2.85
	1/3	5±0.2	0.067	0.62	0.94	1.67	2.95
		7.5±0.3	0.069	0.74	0.95	1.78	3.06
		2.5±0.1	0.042	0.58	0.92	1.6	2.94
	1/6	5±0.2	0.065	0.66	0.97	1.65	2.99
		7.5±0.3	0.073	0.82	0.98	1.76	3.1
		2.5±0.1	0.062	0.62	0.95	1.64	3.01
	1/9	5±0.2	0.081	0.68	1	1.69	3.06
		7.5±0.3	0.094	0.84	1.01	1.8	3.17
B		2.5±0.1	0.027	0.42	0.73	1.23	2.32
	1/3	5±0.2	0.043	0.56	0.84	1.33	2.48
		7.5±0.3	0.062	0.63	0.75	1.42	2.56
		2.5±0.1	0.041	0.49	0.78	1.31	2.16
	1/6	5±0.2	0.058	0.63	0.77	1.23	2.21
		7.5±0.3	0.062	0.78	0.8	1.43	2.43
		2.5±0.1	0.051	0.58	0.72	1.23	2.52
	1/9	5±0.2	0.073	0.64	0.93	1.54	2.66
		7.5±0.3	0.081	0.82	0.95	1.47	2.73
B		2.5±0.1	0.027	0.42	0.73	1.23	2.32
	1/3	5±0.2	0.043	0.56	0.84	1.33	2.48
		7.5±0.3	0.062	0.63	0.75	1.42	2.56
		2.5±0.1	0.041	0.49	0.78	1.31	2.16
	1/6	5±0.2	0.058	0.63	0.77	1.23	2.21
		7.5±0.3	0.062	0.78	0.8	1.43	2.43
		2.5±0.1	0.051	0.58	0.72	1.23	2.52
	1/9	5±0.2	0.073	0.64	0.93	1.54	2.66
		7.5±0.3	0.081	0.82	0.95	1.47	2.73

subside of R_{hi} value is different for each pollution level with an increase in J value. For example, the amount of decreasing R_{hi} value is 6.3% with increased in J from 1 to 8 under ESDD of 0.09 mg/cm^2, while it is 9.7% when ESDD equal to 0.24 mg/cm^2 at the same increment of J. Figure 9(c) shows the relation between the LC index and the severity of pollution under the variation of the z ratio, it can be observed that the effect of increasing the *NSDD* on LC index R_{hi} is low. It should be indicated that differences in the insulator's profile such as leakage distance, diameter, and number of ribs also has a significant effect on the insulator's LC index and electrical properties as well as shown in Figure 9(d).

D. AC FLASHOVER VOLTAGE STRESS RESULTS IN TERMS OF LC INDEX

Before using the LC index (R_{hi}) as a tool (impact) to calculate the occurrence of flashover and the risk rate of contaminated insulator string usage, the relationship between the LC index and flashover voltage per length unit Ec must be identified. The curve fitting of archived experimental data was done using the following exponent expression given by:

$$E_c = a \times R_{hi}^{b} \tag{14}$$

TABLE 4. LC index result under different non-uniform pollution ($J = 5$), z and W_r.

Type	z	W_r (l/h)	ESDD (mg/cm^2)			
			0.03	0.09	0.15	0.24
A		2.5±0.1	0.38	0.73	1.21	2.01
	1/3	5±0.2	0.48	0.83	1.31	2.11
		7.5±0.3	0.59	0.94	1.42	2.22
		2.5±0.1	0.49	0.84	1.39	2.7
	1/6	5±0.2	0.54	0.89	1.44	2.75
		7.5±0.3	0.65	1	1.55	2.86
		2.5±0.1	0.55	0.88	1.46	2.78
	1/9	5±0.2	0.6	0.93	1.51	2.83
		7.5±0.3	0.71	1.04	1.62	2.94
B		2.5±0.1	0.33	0.68	0.98	1.81
	1/3	5±0.2	0.42	0.78	1.04	1.92
		7.5±0.3	0.54	0.86	1.28	1.98
		2.5±0.1	0.46	0.76	1.08	2.64
	1/6	5±0.2	0.51	0.84	1.40	2.53
		7.5±0.3	0.61	0.94	1.48	2.74
		2.5±0.1	0.52	0.83	1.41	2.68
	1/9	5±0.2	0.6	0.93	1.58	2.73
		7.5±0.3	0.68	0.97	1.54	2.84

where a and b are LC index coefficient and exponent respectively which mainly depends on the insulator geometry, pollution level, wetting etc. Generally, from the relationship E_c-R_{hi} given in Figure 10 - 12, it can be noted that there appears to be a general tendency of the Ec fitted lines for both insulator strings under operating condition. In Figure 10 each point shows the mean experimental data of flashover voltage gradient of tested insulator strings as a function of LC index under different wetting rate, $J = 1$ and $z = 1/3$.

According to Figure 10, increasing LC 1ndex (R_{hi}) from 0.55 to 1.57 and 2.85 for the insulator string type A under wetting rate of 2.5 ± 0.1 l/h, reduces the flashover voltage gradient by 3615% and 46.92%, respectively Meanwhile, the changing process of the value of Ec with the rise of LC index at 5±0.2 l/h, and 7.5±0.3 l/h wetting rate levels is similar to that of 2.5±0.1 l/h level. In addition to, increasing the wetting rate level of the polluted insulators, results in drop of the Ec causing the electrical characteristics of the insulator to be weakened. For example, when R_{hi} is 1.5 for type A insulator string, Ec value is decreased by 31.5% and 47.69% with W_r increasing from 2.5 ± 0.1 l/h to 5±0.2 l/h, and 7.5±0.3 l/h, respectively. This indicates that the higher wetting rate has a significant influence on electrical insulator performance and flashover damage. Meanwhile, the flashover voltage gradient E_c of type A insulator string appeared to be lower than E_c of type B insulator string for all cases. It should be noted that the profile features such as the ribs depth and diameter of the insulators will affect the E_c values. To evaluate the influence of changing in ratio of non-soluble deposit density to soluble deposit density (z) on flashover voltage gradient E_c with increasing LC index, an E_c-R_{hi} curve is plotted as shown in Figure 11. Referring Figure 12, it is clearly seen that the E_c value of glass insulator E_c of the glass insulator strings reduces with decrease in z value. Among the

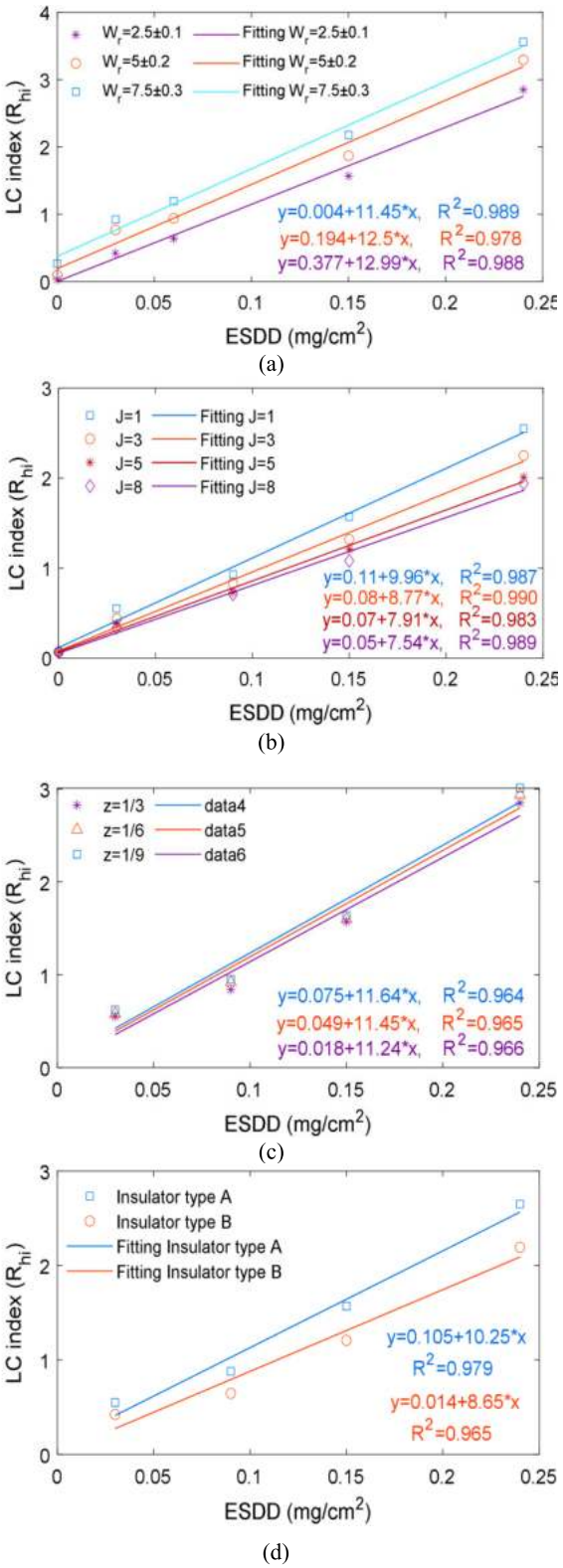

FIGURE 9. The LC index (R_{hi}) as function with ESDD under operation condition: (a) Different *Wr*, (b) Different *J*, (c) Different *z*, (d) Different types of insulators.

tested insulators, the Type A insulator has the most sensitivity to vary the value of z. According to Figure 11, with decreasing the z value from 1/3 to 1/6 and 1/9 for Type B insulator

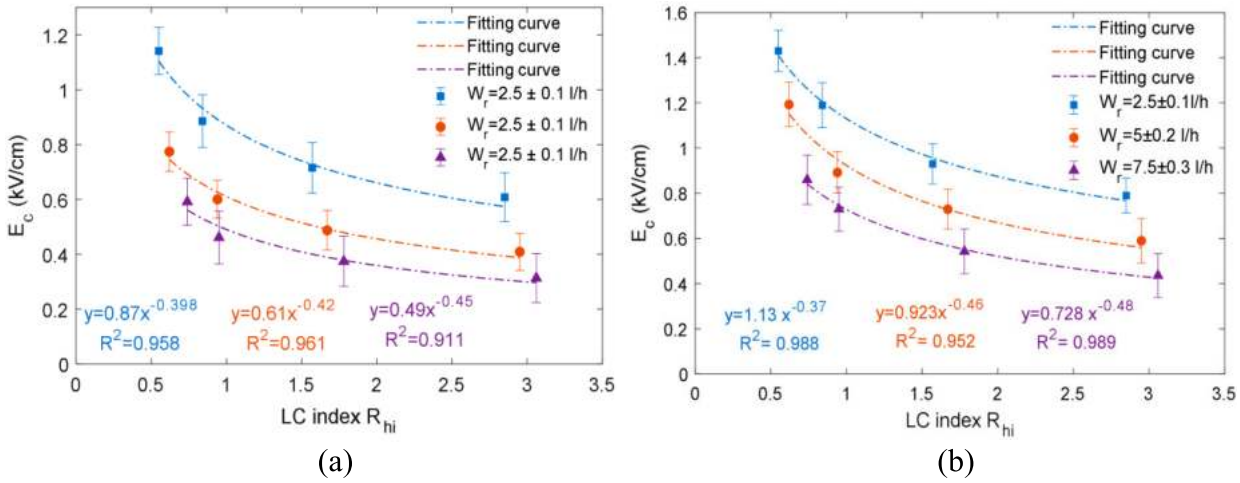

FIGURE 10. *Ec* as function with LC index R_{hi} under $J = 1$, $z = 1/3$ and different wetting rate: (a) Insulator string type A, (b) Insulator string type B.

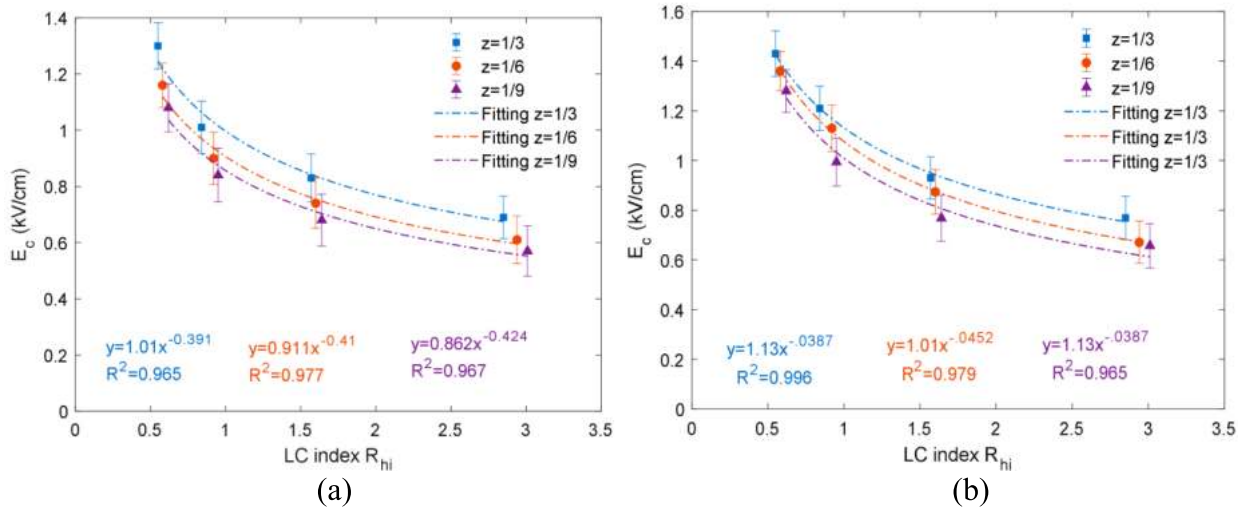

FIGURE 11. *Ec* as function with LC index (R_{hi}) under $Wr = 2.5\pm0.1$ l/h, $J = 1$ and different ratio of NSDD to ESDD: (a) Insulator string type A, (b) Insulator string type B.

string as example with $J = 1$, $W_r = 2.5 \pm 0.1$ l/h and $R_{hi} = 1.5$, the flashover voltage gradient is lessened 5.38% and 12.3%, respectively. Therefore, the effect of the z value on *Ec* decrement is higher at the lesser value of z and by raising the z amount by decreasing *NSDD* amount, this effect is diminished, gradually.

In order to assess the impact of non-uniform pollution distribution on the relationship between E_c and R_{hi}, the E_c curve in terms of R_{hi} under different values of J is plotted in Figure 12. It can be noted from Figure 12 that the non-uniform pollution distribution has a significant effect on the flashover voltage gradient Ec. For example, when W_r is 2.5 ± 0.1 l/h, z is 1/3 and with increasing the value of J by 1 to 3, 5 and 8 for the insulator string A, the E_c increased 30%, 43.1% and 50.8%, respectively. Comparing Figure12 and Figure 13, it can be observed that the influence of raising factor J is more serious than the influence of increasing the parameter z on the flashover voltage gradient of the glass insulators under contamination. It should be concluded from Figure 10, Figure 11 and Figure 12 that the correlation coefficients R^2 of all fitting lines are greater than 0.91, which indicates that the E_c and R_{hi} under operating conditions of both the tested insulators fit the power function well.

IV. PROBABILITY DISTRIBUTION FUNCTIONS PDFS BASED ON LC INDEX

The insulator risk usage using Probability Distribution Functions (PFDs) in terms of ESDD was calculated in [34]. In order to simplify monitoring of insulators' condition, it is deemed extremely useful to have an indicator (a number) that reflects the health condition of the insulators. Accordingly, it would be very useful to calculate the risk and probability of flashover occurrence of the tested insulator based on the index (a number) extracted from Leakage current. As it is known, the risk is defined as the probability multiplied by impact. In this article, the probability will be the density of flashover probability and the impact will become the LC index R_{hi} as indicator of pollution severity. The Probability Distribution

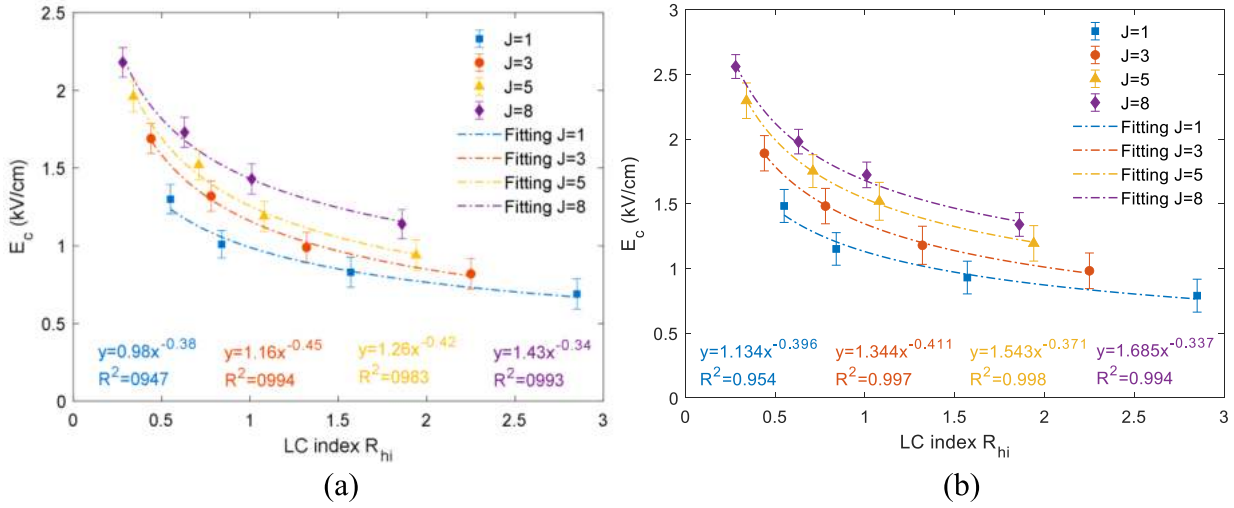

FIGURE 12. *Ec* as function with LC index (R_{hi}) under $Wr = 2.5\pm0.1$ l/h, z = 1/3 and uneven pollution *J*: (a) Insulator string type A, (b) Insulator string type B.

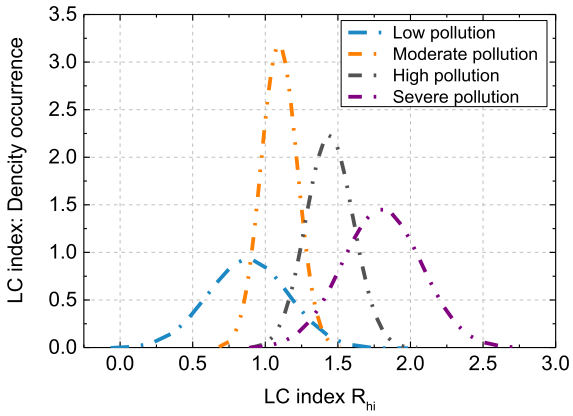

FIGURE 13. LC index existence probability for insulator string.

Functions (PFDs) and a cumulative distribution function have been employed to achieve this purpose. So the requisite PFDs will be the probability of Flashover occurrence as a function of LC index R_{hi} and the probability of LC index R_{hi} existence as a function of this index. According to (15) the flashover occurrence probability can be computed as a function of the LC index as an indicator of the pollution severity.

A. LC INDEX EXISTENCE PROBABILITY

The probability of existence of the LC index can be described by a normal distribution function, expressed as,

$$f(R_{hi}) = \frac{1}{\sigma\sqrt{2\pi}} e^{-\left(\frac{\gamma-\mu}{2\sigma}\right)} \tag{15}$$

γ represents $\ln(R_{hi})$, μ represents $\ln(R_{hi(av)})$ values under the same test and σ represents the standard deviation of $\ln(R_{hi})$. These parameters were calculated using LC index value obtained from test LC of insulator under low, Medium, High and Severe pollution levels. Figure 13 shows the LC index existence probability of each pollution level as a function of the LC index for Type A insulator strings using the Normal Distribution function. The LC index existence probability in normal distribution for both insulator strings is discussed in section C.

B. FLASHOVER OCCURRENCE PROBABILITY BASED ON LC INDEX

Three parameters Weibull distribution function has been utilized for the statistical model of the flashover occurrence and can be represented as [35],

$$P(R_{hi}) = 1 - e^{-\frac{1}{\beta}\left(\left(\frac{R_{hi}}{R_{hi0}}\right)^{\alpha}-1\right)^{k}} \tag{16}$$

$$R_{hi0} = R_{hi(av)} \times \left(\frac{U_0}{U_{av}}\right)^{1/\alpha} \tag{17}$$

$$R_{hi(av)} = \left(\frac{\gamma}{U_C}\right)^{1/\alpha} \tag{18}$$

$$\beta = \frac{n \cdot c}{(1-nc)(ln2)^{1/k}} \tag{19}$$

$$c = \sigma/U_{av} \tag{20}$$

$$k = \frac{1.38}{ln(n/(n-1))} \tag{21}$$

$$U_0 = U_{av} - n\sigma \tag{22}$$

U_0, U_{AV}, U_C, R_{hio}, and $R_{hi(av)}$ are withstand voltage (probability flashover = 0), average flashover voltage, continuous operating voltage. LC index value when flashover probability is zero and the average value of LC index obtained at each pollution level, *k*, α, and γ are constant and n is the constant equal to 2 [34]. The flashover occurrence probability for insulator string Type A with different wetting rate W_r are illustrated in Figure 14, as it clearly seen from Figure 14, the occurrence of flashover increases with increase in wetting rate under constant LC index value.

It can also be noted that by increasing LC index value, the ratio of flashover occurrence probability increases with the rise in wetting rate. According to Figure 14, when LC index equals to 1 for insulator string Type A, the flashover occurrence probability increases by 12% when the W_r increases from 2.5±0.1 l/h to 5±0.2 l/h, whereas, when LC index is 1.5, the flashover occurrence probability rises by 18% in the same increment of W_r.

The flashover occurrence probability under effect of non-uniform pollution distribution based on LC index is

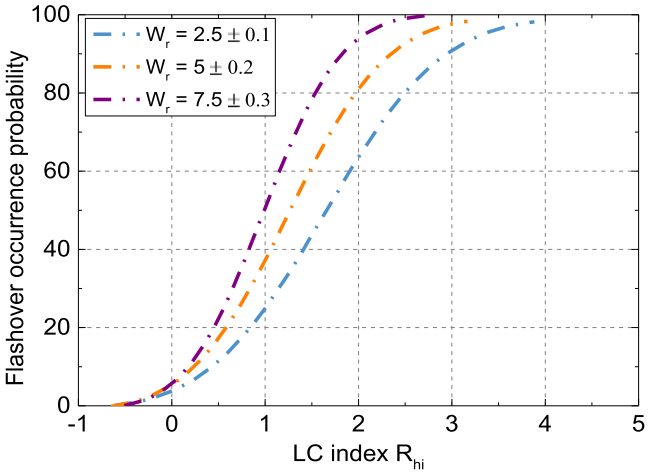

FIGURE 14. Probability of flashover occurrence in terms of LC index for insulator string A in different wetting rate.

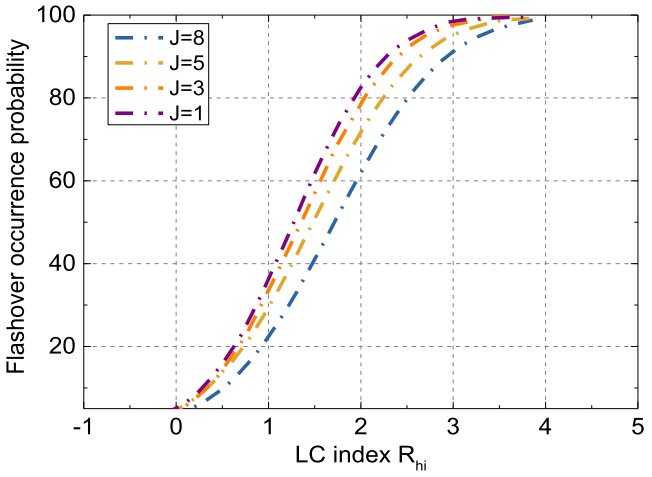

FIGURE 15. Probability of flashover occurrence in terms of LC index for insulator string A with version of *J*.

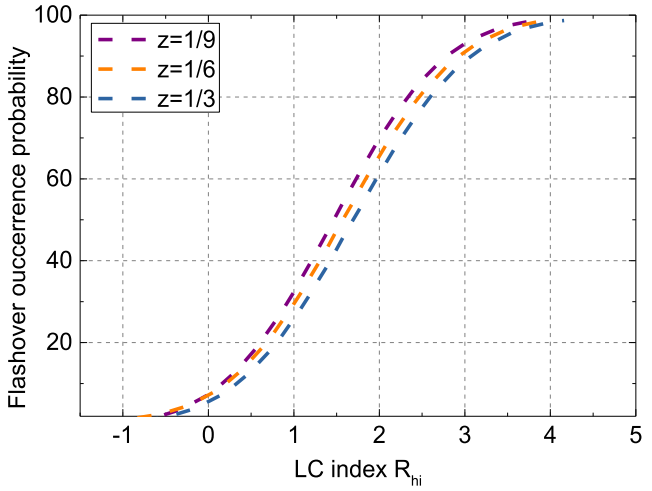

FIGURE 16. Probability of flashover occurrence in terms of LC index for insulator string *A* in z.

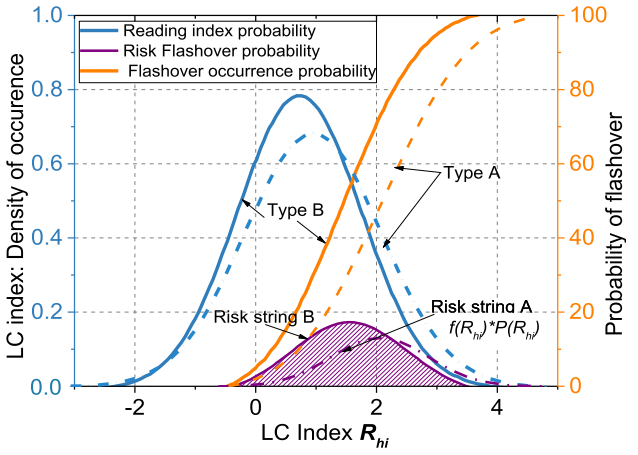

FIGURE 17. Calculation of insulator strings utilization risk.

illustrated in Figure 15. It can be seen that J's effect on flashover occurrence probability is not substantial. Regarding Figure 15, the flashover occurrence probability of insulator string A reduces with rising the value of J. The influence of the increased amount of *NSDD* on flashover occurrence probability is shown in Figure 16. It can be observed with a weak effect corresponding z value compared to the other investigated conditions (J and W_r). Generally, the flashover occurrence probability decreases with increasing z value.

C. CALCULATION OF RISK INSULATOR

As mentioned above, the insulator risk can be defined by multiplying the LC index reading as an indicator of the level of pollution by the probability of flashover occurrence and integral of the curve produced will be the risk of using the insulator as expressed in (23):

$$S = \int_{R_{hi0}}^{R_{hi(FO)}} f(R_{hi}) \times P(R_{hi}) dR_{hi} \tag{23}$$

where S is insulator risk, $f(R_{hi})$ as defined in (15) and $P(R_{hi})$ as defined in (16). Figure 17 shows the risk (S) calculation of both the uniformly polluted insulator strings used under W_r is 2.5±0.1 l / h and z = 1/3.

According to Figure17, the risk of using an insulator string Type A is greater as compared to insulators string type B. In other words, the insulator's Type cup and pin with long leakage distance and thick diameter results in less risk than insulators with short creepage distance and small diameter.

The risk values for the insulators studied are displayed in Figure18 which are 0.12 (p.u) for insulator A and 0.17 (p.u) for insulators A and B, respectively.

To assess the impact of contamination on flashover occurrence risk using the novel LC index, the percentage risk of use of the examined insulators under operating condition have been calculated and demonstrated in Figures 18-21. Figure18 demonstrates the percentage of insulator usage risk as function of LC index in different values of W_r. It can be observed that the insulator risk increases with rising value of W_r. Also, this increase of risk will intensify as the LC index. As a result, the lowest risk will occur at the lowest R_{hi} and wetness levels and the worst risk will be at the highest R_{hi} and wetness levels. Meanwhile, the ratio of insulators risk

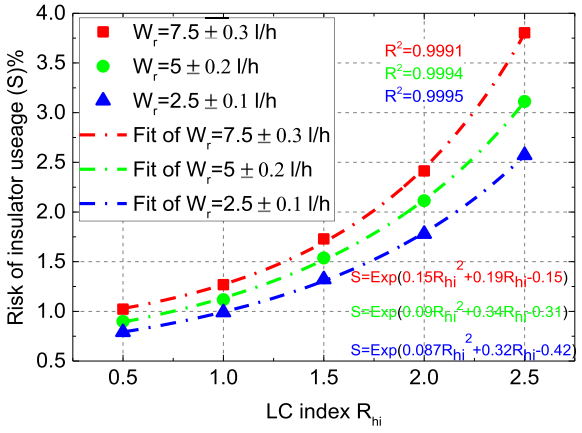

FIGURE 18. Risk of insulator string type A utilization as a function of LC index in different of wetting rate *Wr*, $j = 1$ and $z = 1/3$.

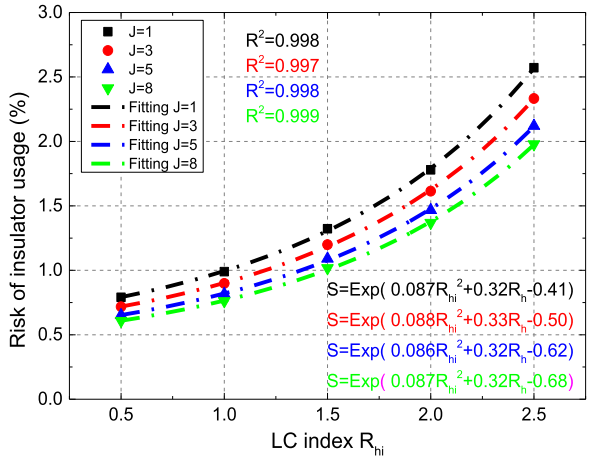

FIGURE 19. Risk of insulator string type A utilization as a function of LC index under non-uniform pollution, *Wr* = 2.5 ± 0.1 l/h and $z = 1/3$.

increased with the increase of *Wr*. Figure 19 shows the risk of the insulator string A as a function with an LC index of non-uniform pollution (different J) under wetting rate of 2.5 ± 0.1 l/h and $z = 1/3$, it can be observed that the increase in J value (increase in ESDD in bottom surface compared with the top surface) leads to a reduced on the risk of insulators. This influence results in a decrease in the conductivity of the insulator surface with an increase in *ESDD* in the bottom surface compared to the top surface. Figure 20 exhibits the risk of insulator string A as a function with an LC index of different z value, it can be found that the decrease in z value (increase in *NSDD*) corresponds to an increase in the risk of insulators. This effect is due to the resulting reduction in insulator surface resistance with an increase in *NSDD*. Figure 21 illustrates the effect of insulator geometric structure in resist of the risk under the same values of LC index. It can be observed that the insulator string type A (thinner diameter and shorter length) are more at risk than insulator string Type B (thicker diameter and longer length). Therefore, the correlation between insulator risk and LC index was assumed as the positive exponent.

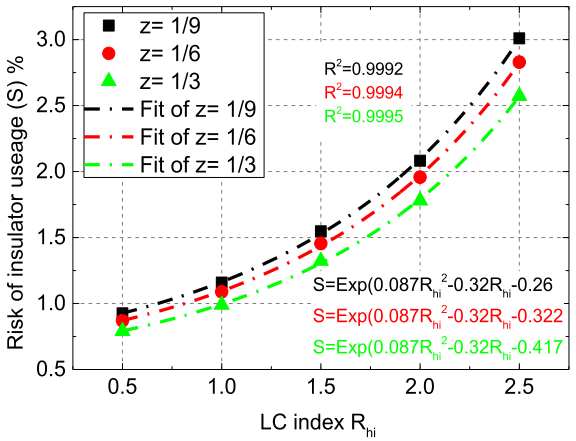

FIGURE 20. Risk of insulator string type A utilization as a function of LC index in different of *z* under *Wr* = 2.5 ± 0.1 l/h and $J = 1$.

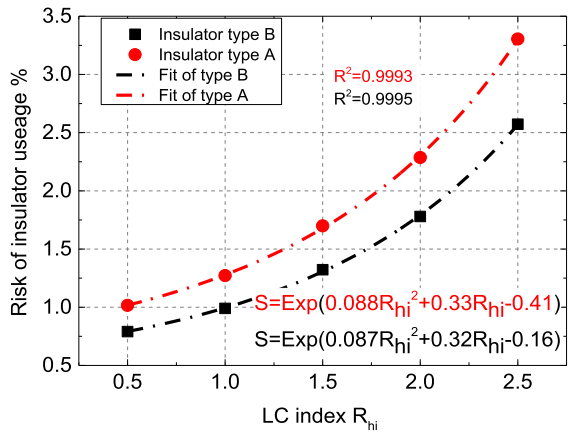

FIGURE 21. Risk of insulator string type A utilization as a function of LC index in different of insulator Type.

The percentage of insulator risk data was fitted with exponent function under the specific LC index values, the best fitting found is formulated as:

$$S = e^{(aR_{hi}^2 + bR_{hi} + c)} \tag{24}$$

where *a, b* and *c* are constants of positive power exponent function, these constants values have been shown on figures. According to Figures 18-21, the fitting curves correlation coefficients R^2 for all lines are greater than 0.97. This indicates that the power function in (24) has the excellent fit to assess the risk of insulators in terms of LC index R_{hi} under operating conditions of both the tested insulators.

V. CONCLUSION

In this article, the risk of two glass insulators with different profiles has been studied. With a variation of the pollution severity, non-uniform distribution pollution, *ESDD* to *NSDD* ratio and the wetting rate has been discussed. For the assist risk insulator under these conditions, a novel LC index derived from the frequency domain of leakage current was used. The proposed index provided, can be used as an effective tool in predicting the contamination severity on

outdoor insulators. The relationship between the flashover voltage gradient and LC index has a negative slope. In other words, the increase of the LC index has an effect on the decreased flashover voltage gradient by increasing J value, decreasing z value, and increasing Wr value. The study carried out in this article suggests the probability distribution function and a cumulative distribution as a function to estimate the insulator risk based on the proposed novel index. Finally, the correlation between LC index and insulator risk has been estimated in an exponent function form. The insulator risk resulted to be positive with increased LC index and affected positively on the risk of the insulator by increasing J value, decreasing z value, and increasing Wr value. The results obtained indicate that the correlation between LC index (R_{hi}) and insulator risk (S) has high accuracy in evaluating the percentage risk value of insulators under test. In conclusion, the results presented in this article are very useful and more accurate in predicting outdoor insulator health and maintain a long life of existing transmission lines. The proposed technique can be a viable solution to estimating the magnitude of contamination on insulators without the direct measurement. In addition, it may also be effectively applied online on any type of insulators in an effort to estimate the degree of exposure and the probability of flashover on outdoor insulators.

REFERENCES

[1] Y. Liu, X. Kong, B. Du, J. Li, and J. Sun, "Numerical investigation on collision of pollution particles on outdoor insulators," *IEEE Access*, vol. 7, pp. 56974–56985, 2019.

[2] Z. Li, Z. Yang, and B. Du, "Surface charge transport characteristics of ZnO/silicone rubber composites under impulse superimposed on DC voltage," *IEEE Access*, vol. 7, pp. 3008–3017, 2019.

[3] M. Ramesh, L. Cui, and R. S. Gorur, "Electrical power and energy systems impact of superficial and internal defects on electric field of composite insulators," *Int. J. Electr. Power Energy Syst.*, vol. 106, no. 6, pp. 327–334, 2019.

[4] X. Zhang, J. Zhu, S. Bu, Q. Li, V. J. Terzija, and S. M. Rowland, "The development of low-current surface arcs under clean and salt-fog conditions in electricity distribution networks," *IEEE Access*, vol. 6, pp. 15835–15843, 2018.

[5] M. Douar, A. Beroual, and X. Souche, "Degradation of various polymeric materials in clean and salt fog conditions: Measurements of AC flashover voltage and assessment of surface damages," *IEEE Trans. Dielectr. Electr. Insul.*, vol. 22, no. 1, pp. 391–399, Feb. 2015.

[6] Z. Zhang, X. Liu, X. Jiang, J. Hu, and D. W. Gao, "Study on AC flashover performance for different types of porcelain and glass insulators with non-uniform pollution," *IEEE Trans. Power Del.*, vol. 28, no. 3, pp. 1691–1698, Jul. 2013.

[7] J. Wardman, T. Wilson, S. Hardie, and P. Bodger, "Influence of volcanic ash contamination on the flashover voltage of HVAC outdoor suspension insulators," *IEEE Trans. Dielectr. Electr. Insul.*, vol. 21, no. 3, pp. 1189–1197, Jun. 2014.

[8] A. A. Salem, R. Abd-Rahman, M. S. Kamarudin, and N. A. Othman, "Factors and models of pollution flashover on high voltage outdoor insulators: Review," in *Proc. IEEE Conf. Energy Convers. (CENCON)*, Oct. 2017, pp. 241–246.

[9] Z. Shihua, J. Xingliang, Z. Zhijin, and H. Jianlin, "Flashover voltage prediction of polluted glass insulators based on the characteristics of leakage current," (in Chinese), *Power Syst. Technol.*, vol. 38, no. 2, pp. 440–447, Feb. 2014.

[10] L. Ye, W. Zhou, S. Yang, L. Li, and J. Yu, "Effects of contaminations on voltage distribution along insulator string," *High Voltage App.*, vol. 15, no. 9, pp. 103–108, Sep. 2015.

[11] N. Bashir and H. Ahmad, "Odd harmonics and third to fifth harmonic ratios of leakage currents as diagnostic tools to study the ageing of glass insulators," *IEEE Trans. Dielectr. Electr. Insul.*, vol. 17, no. 3, pp. 819–832, Jun. 2010.

[12] T. Las, V. M. Moreno, R. S. Gorur, and A. Kroese, "Impact of corona on the long-term performance of nonceramic insulators," *IEEE Trans. Dielectr. Electr. Insul.*, vol. 11, no. 5, pp. 913–915, Oct. 2004.

[13] Y. Liu, X. Kong, Y. Wu, and B. Du, "Dynamic behavior of droplets and flashover characteristics for CFD and experimental analysis on SiR composites," *IEEE Access*, vol. 7, pp. 8095–8101, 2019.

[14] N. Dhahbi-Megriche and A. Béroual, "Time-frequency analyses of leakage current waveforms of high voltage insulators in uniform and non-uniform polluted conditions," *IET Sci. Meas. Technol.*, vol. 9, pp. 1–10, Jul. 2015.

[15] A. A. Salem, R. Abd-Rahman, M. S. Kamarudin, H. Ahmad, N. A. Jamail, N. A. Othman, M. T. Ishak, M. N. Baharom, and S. Al-Ameri, "Proposal of a dynamic numerical approach in predicting flashover critical voltage," *Int. J. Power Electron. Drive Syst.*, vol. 10, no. 2, p. 602. 2019.

[16] A. H. El-Hag, S. H. Jayaram, and E. A. Cherney, "Fundamental and low frequency harmonic components of leakage current as a diagnostic tool to study aging of RTV and HTV silicone rubber in salt-fog," *IEEE Trans. Dielectr. Electr. Insul.*, vol. 10, no. 1, pp. 128–136, Feb. 2003.

[17] A. A. Salem, R. Abd-Rahman, H. Ahmad, M. S. Kamarudin, N. A. M. Jamal, N. A. Othman, and M. T. Ishak, "A new flashover prediction on outdoor polluted insulator using leakage current harmonic components," in *Proc. IEEE 7th Int. Conf. Power Energy (PECon)*, Dec. 2018, pp. 413–418.

[18] C. N. Richards and J. D. Renowden, "Development of a remote insulator contamination monitoring system," *IEEE Trans. Power Del.*, vol. 12, no. 1, pp. 389–397, Jan. 1997.

[19] R. Abd-Rahman, A. Haddad, N. Harid, and H. Griffiths, "Stress control on polymeric outdoor insulators using zinc oxide microvaristor composites," *IEEE Trans. Dielectr. Electr. Insul.*, vol. 19, no. 2, pp. 705–713, Apr. 2012.

[20] E. Fontana, J. F. Martins-Filho, S. C. Oliveira, F. J. M. M. Cavalcanti, R. A. Lima, G. O. Cavalcanti, T. L. Prata, and R. B. Lima, "Sensor network for monitoring the state of pollution of high-voltage insulators via satellite," *IEEE Trans. Power Del.*, vol. 27, no. 2, pp. 953–962, Apr. 2012.

[21] B. Moula, A. Mekhaldi, M. Teguar, and A. Haddad, "Characterization of discharges on non-uniformly polluted glass surfaces using a wavelet transform approach," *IEEE Trans. Dielectr. Electr. Insul.*, vol. 20, no. 4, pp. 1457–1466, Aug. 2013.

[22] Y. Kemari, A. Mekhaldi, and M. Teguar, "Experimental investigation and signal processing techniques for degradation assessment of XLPE and PVC/B materials under thermal aging," *IEEE Trans. Dielectr. Electr. Insul.*, vol. 24, no. 4, pp. 2559–2569, 2017.

[23] M. Douar, A. Mekhaldi, and M. Bouzidi, "Flashover process and frequency analysis of the leakage current on insulator model under non-uniform pollution conditions," *IEEE Trans. Dielectr. Electr. Insul.*, vol. 17, no. 4, pp. 1284–1297, Aug. 2010.

[24] M. F. Palangar and M. Mirzaie, "Diagnosis porcelain and glass insulators conditions using phase angle index based on experimental tests," *IEEE Trans. Dielectr. Electr. Insul.*, vol. 23, no. 3, pp. 1460–1466, Jun. 2016.

[25] Z. Sahli, A. Mekhaldi, R. Boudissa, and S. Boudrahem, "Prediction parameters of dimensioning of insulators under non-uniform contaminated conditions by multiple regression analysis," *Electr. Power Syst. Res.*, vol. 81, no. 4, pp. 821–829, Apr. 2011.

[26] L. Lan, G. Zhang, Y. Wang, X. Wen, W. Wang, and H. Pei, "The influence of natural contamination on pollution flashover voltage waveform of porcelain insulators in heavily polluted area," *IEEE Access*, vol. 7, pp. 121395–121406, 2019.

[27] H. Terrab and A. Bayadi, "Experimental study using design of experiment of pollution layer effect on insulator performance taking into account the presence of dry bands," *IEEE Trans. Dielectr. Electr. Insul.*, vol. 21, no. 6, pp. 2486–2495, Dec. 2014.

[28] J. Li, W. Sima, C. Sun, and S. Sebo, "Use of leakage currents of insulators to determine the stage characteristics of the flashover process and contamination level prediction," *IEEE Trans. Dielectr. Electr. Insul.*, vol. 17, no. 2, pp. 490–501, Apr. 2010.

[29] T. Suda, "Frequency characteristics of leakage current waveforms of a string of suspension insulators," *IEEE Trans. Power Del.*, vol. 20, no. 1, pp. 481–487, Jan. 2005.
[30] A. H. El-Hag, "Leakage current characterization for estimating the conditions of non-ceramic insulators' surfaces," *Electr. Power Syst. Res.*, vol. 77, nos. 3–4, pp. 379–384, Mar. 2007.
[31] H. Kordkheili, H. Abravesh, M. Tabasi, M. Dakhem, and M. Abravesh, "Determining the probability of flashover occurrence in composite insulators by using leakage current harmonic components," *IEEE Trans. Dielectr. Electr. Insul.*, vol. 17, no. 2, pp. 502–512, Apr. 2010.
[32] A. A. Salem, R. Abd-Rahman, S. Ahmed Al-Gailani, M. S. Kamarudin, H. Ahmad, and Z. Salam, "The leakage current components as a diagnostic tool to estimate contamination level on high voltage insulators," *IEEE Access*, vol. 8, pp. 92514–92528, 2020.
[33] M. Rezaei, A. Mostajabi, I. A. Joneidi, and N. G. Alvijeh, "Experimental and simulation study on leakage current of ceramic insulator under heavy pollution environment," in *Proc. 32nd Power Syst. Conf.*, 2017, pp. 1–5.
[34] A. Tzimas and S. M. Rowland, "Risk estimation of ageing outdoor composite insulators with Markov models," *IET Gener., Transmiss. Distrib.*, vol. 6, no. 8, pp. 803–810. 2012.
[35] M. El-Shahat and H. Anis, "Risk assessment of desert pollution on composite high voltage insulators," *J. Adv. Res.* vol. 5, no. 5, pp. 569–576, 2014.

ALI AHMED SALEM (Member, IEEE) received the M.Eng. degree in electrical power engineering from Universiti Tun Hussein Onn Malaysia (UTHM), in 2016, where he is currently pursuing the Ph.D. degree in high voltage with the Faculty of Electrical Engineering. His research interest includes the dynamic arc modeling of pollution flashover on high-voltage outdoor insulators.

RAHISHAM ABD-RAHMAN (Member, IEEE) received the M.Eng. degree in electrical and electronic engineering and the Ph.D. degree in high voltage from Cardiff University, U.K., in 2008 and 2012, respectively. He is currently a Senior Lecturer with the Faculty of Electrical and Electronic Engineering, Universiti Tun Hussein Onn Malaysia (UTHM). He is also a Chartered Engineer (C.Eng.) at U.K. His research interests include dielectric materials, outdoor insulator, and discharge phenomenon. He is also a member of engineering institutions, such as IET (MIET), and the Board of Engineers Malaysia (BEM).

SAMIR AHMED AL-GAILANI (Member, IEEE) received the B.Sc. degree (Applied) from the Higher Technical institute, Aden, Yemen, in 1992, and the Ph.D. degree in optoelectronics from Universiti Teknologi Malaysia (UTM), in 2014. He started his career as a Senior Lecturer with the Higher Technical institute. Since after completing his Ph.D. degree, has been given various responsibilities, including teaching, postdoctoral fellow, supervising laboratory sessions, supervising post-graduate students and undergraduate students, academic advisor, head of laboratory, head of research group, chairman and member of different committees, and conducting short courses and training. He has authored 20 ISI articles, has an H-index of 7 and total citations of 212, and presented more than 90 papers in reputed refereed conferences. He also successfully supervised nine undergraduate students. He received the Best Student Award for his Ph.D. degree.

ZAINAL SALAM received the B.Sc. degree in electronics engineering from California State University, Chico, CA, USA, in 1985, the M.E.E. degree in electrical engineering from Universiti Teknologi Malaysia (UTM), Kuala Lumpur, Malaysia, in 1989, and the Ph.D. degree in power electronics from the University of Birmingham, Birmingham, U.K., in 1997. He is currently a Professor in Power Electronics and Renewable Energy with the Centre of Electrical Energy Systems, Faculty of Electrical Engineering, UTM. He represents the country as an Expert for the International Energy Agency PV Power Systems Task 13 Working Group, which focuses on the reliability and performance of photovoltaic power systems. His main research interests include all areas of design, instrumentation, and control of power electronics and renewable energy systems. He is also the Vice Chair of the IEEE Power Electronics, Industrial Electronics and Industry Application Joint Chapter, Malaysia Section, from 2011 to 2013 and in 2016. From 2011 to 2013, he was the Editor of the IEEE TRANSACTIONS ON SUSTAINABLE ENERGY.

MUHAMMAD SAUFI KAMARUDIN (Member, IEEE) received the B.Eng. and M.Eng. degrees in electrical engineering (power) from Universiti Teknologi Malaysia (UTM), in 2003 and 2005, respectively, and the Ph.D. degree in high voltage engineering from Cardiff University, U.K., in 2014. He is currently a Senior Lecturer with the Faculty of Electrical and Electronic Engineering, Universiti Tun Hussein Onn Malaysia (UTHM). His research interests include gas discharges, high-voltage surge arresters, and dielectrics and electrical insulation systems. He is also a Registered Member of the Board of Engineers Malaysia (BEM). He is also a Graduate Member of the Institution of Engineers, Malaysia (IEM).

HIDAYAT ZAINUDDIN (Member, IEEE) received the bachelor's degree in electrical engineering from Universiti Teknologi Malaysia, in 2003, the M.Sc. degree in electrical power engineering with business from the University of Strathclyde, Glasgow, in 2005, and the Ph.D. degree from the University of Southampton, in 2013. He has been serving as an Academic Staff with Universiti Teknikal Malaysia Melaka, since 2003, where he is currently appointed as a Senior Lecturer with the Faculty of Electrical Engineering. He is also serving as the Head of the High Voltage Engineering Research Laboratory, Universiti Teknikal Malaysia Melaka. His research interests include high-voltage equipment and insulation condition monitoring, failure analysis, and power system protection coordination.

MOHD FAIROUZ MOHD YOUSOF (Member, IEEE) received the B.Eng. and M.Eng. degrees from Universiti Teknologi Malaysia and the Ph.D. degree from The University of Queensland, Australia, in 2015. He was appointed as a Visiting Researcher at the TNB Research, from 2018 to 2019. He has been a Principal Consultant at Xair Energy Sdn Bhd, since 2019. He is currently a Lecturer with the Department of Electrical Power Engineering, Universiti Tun Hussein Onn Malaysia (UTHM). His main research interests include condition-based monitoring and assessment of high-voltage equipment specifically power transformer and rotating machine. He is also a Registered Member of the Board of Engineers Malaysia (BEM) and a member of the Malaysian Society for Engineering and Technology (MySET).